Journal of Solid State Chemistry **151,** 317–322 (2000)
doi:10.1006/jssc.2000.8661, available online at http://www.idealibrary.com on IDEAL®

Syntheses and Structures of the New Quaternary Rubidium Selenides RbLn_2CuSe$_4$ (Ln = Sm, Gd, Dy), Rb$_{1.5}Ln_2$Cu$_{2.5}$Se$_5$ (Ln = Gd, Dy), and RbSm$_2$Ag$_3$Se$_5$

Fu Qiang Huang and James A. Ibers

Department of Chemistry, Northwestern University, 2145 Sheridan Road, Evanston, Illinois 60208-3113

Received January 11, 2000; accepted February 18, 2000

Six quaternary rubidium selenides RbLn_2CuSe$_4$ (Ln = Sm, Gd, Dy), Rb$_{1.5}Ln_2$Cu$_{2.5}$Se$_5$ (Ln = Gd, Dy), and RbSm$_2$Ag$_3$Se$_5$ have been synthesized at 1073 K with the use of a reactive flux of Rb$_2$Se$_3$. At 153 K all compounds contain four formula units in orthorhombic unit cells. The isostructural compounds RbLn_2CuSe$_4$ crystallize in space group *Cmcm*; the isostructural compounds Rb$_{1.5}Ln_2$Cu$_{2.5}$Se$_5$ crystallize in space group *Pnnm*; RbSm$_2$Ag$_3$Se$_5$ crystallizes in space group *Cmcm*. The cells of RbLn_2CuSe$_4$ are (Ln, a, b, c (Å)): Sm, 4.1834(9), 14.308(3), 14.439(3); Gd, 4.1568(8), 14.227(3), 14.409(3); Dy, 4.1237(10), 14.083(4), 14.291(3), and the corresponding R_1 indices for the refined structures are 0.023, 0.029, and 0.039. The cells of Rb$_{1.5}Ln_2$Cu$_{2.5}$Se$_5$ are: Gd, 16.243(3), 16.449(3), 4.0980(7); Dy, 16.120(3), 16.292(3), 4.0610(8), and the R_1 indices are 0.036 and 0.043. The cell of RbSm$_2$Ag$_3$Se$_5$ is 4.3223(6), 15.229(2), 17.420(3) Å and the R_1 index is 0.025. All six are closely related three-dimensional tunnel structures. Their anionic frameworks are built from LnSe$_6$ octahedra and MSe$_4$ (M = Cu, Ag) tetrahedra. RbLn_2CuSe$_4$ contains infinite $^1_\infty$[CuSe$_3$] chains of vertex-sharing tetrahedra; Rb$_{1.5}Ln_2$Cu$_{2.5}$Se$_5$ also contains infinite chains of tetrahedra; and the tunnel in RbSm$_2$Ag$_3$Se$_5$ holds one Rb$^+$ cation in a 10-membered ring consisting of six Ag–Se bonds and four Sm–Se bonds. Rb$_{1.5}$Dy$_2$Cu$_{2.5}$Se$_5$, which is paramagnetic, obeys the Curie–Weiss law and has an effective magnetic moment of 10.63(4) μ_B. © 2000 Academic Press

INTRODUCTION

Quaternary lanthanides and actinides that contain a *d*-block metal in addition to the *f*-block metal are of interest because intriguing structural and physical properties may result from the interplay of covalent transition-metal and the more ionic lathanide and actinide bonding. The high-T_c cuprate superconductors provide a spectacular example. Recently, a number of $A/Ln/M/Q$ (A = alkali or earth-alkaline metal; Ln = *f*-block element, usually a rare earth; M = *d*-block element; Q = chalcogen = S, Se, Te) systems have been synthesized. These include CsUTiTe$_5$ (1), Ba$LnMQ_3$ (Ln = rare-earth; M = Cu, Ag, Au; Q = S, Se, Te) (2–5), Ba$_2Ln$Ag$_5$S$_6$ (Ln = La, Y) (6), K$_{1.5}$Dy$_2$Cu$_{2.5}$Te$_5$ (5), K$_{0.5}$Ba$_{0.5}$DyCu$_{1.5}$Te$_3$ (5), KGd$_2$CuS$_4$ (7), K$_2$CeCu$_2$S$_4$ (8), ALnCu$_2$S$_6$ (A = K, Cs; Ln = La, Ce, Eu) (8–10), ALnCuQ_3 (A = K, Cs; Ln = Ce, U; Q = S, Se, Te) (1, 10), K$_2$CeAg$_3$Te$_4$ (11), KCeCuTe$_4$ (12), and Rb$_2$CeCu$_3$Te$_5$ (13). These compounds crystallize in a variety of structure types that include two-dimensional layered structures and three-dimensional tunnel structures. The M atoms (except Ti) are tetrahedrally coordinated by chalcogen atoms. These tetrahedra enter into chains, layers, and other frameworks. Here we report the synthesis and structural characterization of six new compounds containing *f*- and *d*-block metals, namely the quaternary rubidium selenides RbLn_2CuSe$_4$ (Ln = Sm, Gd, Dy), Rb$_{1.5}Ln_2$Cu$_{2.5}$Se$_5$ (Ln = Gd, Dy), and RbSm$_2$Ag$_3$Se$_5$.

EXPERIMENTAL

Syntheses

The following reagents were used as obtained: Rb (Aldrich, 98 + %), Sm (Alfa, 99.9%), Gd (Alfa, 99.9%), Dy (Aldrich, 99.9%), Cu (Aldrich, 99.999%), Ag (Alfa, 99.99%), Se (Aldrich, 99.5%). Rb$_2$Se$_3$, the reactive flux (14) employed in the syntheses, was prepared by the stoichiometric reaction of the elements in liquid NH$_3$. The reaction mixtures were (Rb$_2$Se$_3$, Ln, Cu or Ag, Se in mmol): RbLn_2CuSe$_4$ (1.2, 1.0, 0.5, 2.0); Rb$_{1.5}Ln_2$Cu$_{2.5}$Se$_5$ (1.2, 1.0, 1.0, 2.0); RbSm$_2$Ag$_3$Se$_5$ (1.2, 1.0, 1.0, 3.0). These mixtures were loaded into fused-silica tubes under an Ar atmosphere in a glove box. These tubes were sealed under a 10^{-4} Torr atmosphere and then placed in a computer-controlled furnace. The samples were heated to 1073 K in 15 h, kept at 1073 K for 30 h, and then cooled to 298 K in 10 h. Major products in all instances were red needles of the desired materials. Yields varied from 70 to 90%. Selected single crystals were examined with an EDX-equipped Hitachi S-4500 SEM and were found to have the stated compositions within the accuracy

0022-4596/00 $35.00

TABLE 1

Crystal Data and Structure Refinement for RbLn_2CuSe$_4$ (Ln = Sm, Gd, Dy), $Rb_{1.5}Ln_2Cu_{2.5}Se_5$ (Ln = Gd, Dy), and $RbSm_2Ag_3Se_5$

Compound	$RbSm_2CuSe_4$	$RbGd_2CuSe_4$	$RbDy_2CuSe_4$	$Rb_{1.5}Gd_2Cu_{2.5}Se_5$	$Rb_{1.5}Dy_2Cu_{2.5}Se_5$	$RbSm_2Ag_3Se_5$
Formula weight	765.55	779.35	789.85	996.36	1006.86	1104.58
a (Å)	4.1834(9)	4.1568(8)	4.1237(10)	16.243(3)	16.120(3)	4.3223(6)
b (Å)	14.308(3)	14.227(3)	14.083(4)	16.449(3)	16.292(3)	15.229(2)
c (Å)	14.439(3)	14.409(3)	14.291(3)	4.0980(7)	4.0610(8)	17.420(3)
Space group	*Cmcm*	*Cmcm*	*Cmcm*	*Pnnm*	*Pnnm*	*Cmcm*
Z	4	4	4	4	4	4
T (K)	153	153	153	153	153	153
Volume	864.3(3)	852.2(3)	830.0(3)	1094.9(3)	1066.5(4)	1146.6(3)
λ (Å)	0.71073	0.71073	0.71073	0.71073	0.71073	0.71073
ρ_c (g/cm^3)	5.883	6.075	6.321	6.044	6.271	6.399
μ (cm^{-1})	381.90	405.18	436.27	399.12	425.51	351.40
Transmission factors	0.07–0.50	0.04–0.31	0.06/0.54	0.13–0.56	0.04–0.36	0.06–0.41
Total reflections/unique	3876/620	2311/602	1136/520	6750/1552	7342/1504	5196/831
R_1[a]	0.023	0.029	0.039	0.036	0.043	0.025
wR_2[b]	0.059	0.069	0.087	0.079	0.095	0.060

[a] $R_1 = \sum ||F_o| - |F_c|| / |F_o|$; $F_o^2 > 2\sigma(F_o^2)$.

[b] $wR_2 = \{\sum [w(F_o^2 - F_c^2)^2] / \sum wF_o^4\}^{1/2}$; $w^{-1} = \sigma^2(F_o^2) + (0.04 \times F_o^2)^2$ for $F_o^2 \geq 0$ and $w^{-1} = \sigma^2(F_o^2)$ for $F_o^2 < 0$.

of the method (±5%). All these compounds are modestly stable in air.

Crystallography

Single-crystal X-ray diffraction data were obtained with the use of graphite-monochromatized Mo$K\alpha$ radiation (λ = 0.71073 Å) at 153 K on a Bruker Smart-1000 CCD diffractometer (15). Intensity data were collected with the program SMART (15). Cell refinement and data reduction were carried out with the use of the program SAINT (15) and face-indexed absorption corrections were carried out numerically with the program XPREP (16). Then the program SADABS (15) was employed to make incident beam and decay corrections.

The structures were solved with the direct methods program SHELXS and refined with the full-matrix least-squares program SHELXL of the SHELXTL-PC suite of programs (16). Each final refinement included anisotropic displacement parameters. A secondary extinction correction was included for all but $Rb_{1.5}Gd_2Cu_{2.5}Se_5$.

Refinements of the structures of RbLn_2CuSe$_4$ (Ln = Sm, Gd, Dy) and $RbSm_2Ag_3Se_5$ were straightforward, whereas those of the structures of $Rb_{1.5}Ln_2Cu_{2.5}Se_5$ (Ln = Gd, Dy) were not. In these latter isostructural compounds there are three crystallographically independent Cu sites. Initial isotropic refinements resulted in displacement parameters of the Cu3 atoms that were much larger than those for atoms Cu2 and Cu1. Accordingly, the occupancies of all three Cu sites were varied in a refinement that involved anisotropic displacement parameters. The resultant occupancies of Cu1, Cu2, and Cu3 in the Dy compound were 1.000(8), 0.862(8), and 0.650(9), and in the Gd compound they were 0.992(7), 0.935(7), and 0.559(7). In the final refinements the occupancy of Cu1 was fixed at 1.0 in both structures and the occupancies of Cu2 and Cu3 were varied. The resultant compositions are $Rb_{1.5}Gd_2Cu_{2.496(5)}Se_5$ and $Rb_{1.5}Dy_2Cu_{2.512(6)}$

TABLE 2

Atomic Coordinates[a] and Equivalent Isotropic Displacement Parameters for $RbSm_2CuSe_4$, $RbGd_2CuSe_4$, and $RbDy_2CuSe_4$

Atom	y	z	U_{eq}[b]
$RbSm_2CuSe_4$			
Rb	0.10941(7)	0.25	0.0125(2)
Sm	0.36564(2)	0.06258(2)	0.00808(15)
Cu	0.83772(9)	0.25	0.0115(3)
Se1	0.26338(5)	0.61158(4)	0.00831(18)
Se2	0.43016(7)	0.25	0.0082(2)
Se3	0	0	0.0103(2)
$RbGd_2CuSe_4$			
Rb	0.10992(8)	0.25	0.0106(3)
Gd	0.36565(3)	0.06311(3)	0.00678(19)
Cu	0.83736(11)	0.25	0.0104(3)
Se1	0.26354(6)	0.61072(5)	0.0071(2)
Se2	0.43027(8)	0.25	0.0068(3)
Se3	0	0	0.0090(3)
$RbDy_2CuSe_4$			
Rb	0.11032(17)	0.25	0.0117(5)
Dy	0.36583(6)	0.06309(5)	0.0082(3)
Cu	0.8366(2)	0.25	0.0105(6)
Se1	0.26343(12)	0.60949(11)	0.0085(4)
Se2	0.43042(17)	0.25	0.0087(5)
Se3	0	0	0.0097(5)

[a] The x coordinate of all atoms is 0.

[b] U_{eq} is defined as one third of the trace of the orthogonalized U_{ij} tensor.

Se_5. As there are no close Se ⋯ Se interactions the oxidation states of +1, +3, +1, and −2 for Rb, *Ln*, Cu, and Se, respectively, may be assigned and charge balance is achieved. Additional crystallographic details are given in Table 1. Tables 2, 3, and 4 give positional parameters and equivalent isotropic displacement parameters, and Tables 5, 6, and 7 present selected bond distances for $RbLn_2CuSe_4$ (*Ln* = Sm, Gd, Dy), $Rb_{1.5}Ln_2Cu_{2.5}Se_5$ (*Ln* = Gd, Dy), and $RbSm_2Ag_3Se_5$, respectively.

Magnetic Susceptibility

A 24-mg sample of $Rb_{1.5}Dy_2Cu_{2.5}Se_5$ containing single crystals was used for magnetic susceptibility measurements. Composition of the sample was verified by EDX measurements. The magnetization was measured at 200 G between 5 and 300 K with the use of a Quantum Design SQUID magnetometer. All measurements were corrected for core diamagnetism (17).

RESULTS AND DISCUSSION

The structure of the compounds $RbLn_2CuSe_4$ (*Ln* = Sm, Gd, Dy) (Fig. 1) is isostructural to KGd_2CuS_4 (7). The structure has a three-dimensional tunnel framework. The tunnel, comprising 10-membered rings of four Cu–Se bonds and six *Ln*–Se bonds, is only large enough in cross section to accommodate one Rb^+ cation. The anionic $[Ln_2CuSe_4^-]$ framework is built up from $LnSe_6$ octahedra and $CuSe_4$ tetrahedra. As shown in Fig. 2, there are one-dimensional vertex-sharing $CuSe_4$ tetrahedra running along the [100] direction. This one-dimensional chain can also be found in the $KZrCuS_3$ structure type (18), for example in $BaDyCuTe_3$ (5) (Fig. 3). But $BaDyCuTe_3$ is a layered structure that contains ${}^{2}_{\infty}[DyCuTe_3^{2-}]$ layers separated by Ba^{2+} cations. The ${}^{2}_{\infty}[DyCuTe_3^{2-}]$ layer is built up from $DyTe_7$ monocapped trigonal prisms and $CuTe_4$ tetrahedra alternating along the [100] direction. If the Se3 atom in $RbLn_2CuSe_4$ were broken into two atoms, then the structure would be made up of zigzag ${}^{2}_{\infty}[Ln_2CuSe_5^{3-}]$ layers comprising two edge-sharing $LnSe_6$ octahedra and one $CuSe_4$ tetrahedron in turn along the [001] direction in Fig. 1. Some rules for the edge-sharing of octahedra and tetrahedra to form a two-dimensional layer have been described in the investigation of the *A*/*M*/Cu/*Q* (*A* = Na, K, Cs, Tl; *M* = Ti, Zr; *Q* = S, Se, Te) system (19).

TABLE 3
Atomic Coordinates and Equivalent Isotropic Displacement Parameters for $Rb_{1.5}Gd_2Cu_{2.5}Se_5$ and $Rb_{1.5}Dy_2Cu_{2.5}Se_5$

Atom	*x*	*y*	*z*	U_{eq}
$Rb_{1.5}Gd_2Cu_{2.5}Se_5$				
Rb1	0.32727(8)	0.32569(8)	0	0.0125(3)
Rb2	0	0	0.5	0.0148(4)
Gd1	0.21354(4)	0.55580(4)	0	0.01026(17)
Gd2	0.56197(4)	0.22016(4)	0	0.00999(17)
Cu1	0.15104(10)	0.14669(10)	0	0.0127(4)
Cu2[a]	0.56954(13)	0.03371(12)	0	0.0209(7)
Cu3[b]	0.0215(2)	0.5730(2)	0	0.0190(11)
Se1	0.00189(9)	0.18005(8)	0	0.0095(3)
Se2	0.28345(8)	0.70936(8)	0	0.0093(3)
Se3	0.18177(8)	0 2(8)	0	0.0092(3)
Se4	0.12313(8)	0.39845(8)	0	0.0097(3)
Se5	0.40950(8)	0.11135(8)	0	0.0100(3)
$Rb_{1.5}Dy_2Cu_{2.5}Se_5$				
Rb1	0.32772(9)	0.32581(9)	0	0.0128(3)
Rb2	0	0	0.5	0.0159(5)
Dy1	0.21403(4)	0.55744(5)	0	0.01153(19)
Dy2	0.56196(5)	0.21868(4)	0	0.01138(19)
Cu1	0.15071(12)	0.14741(12)	0	0.0133(4)
Cu2[c]	0.57019(16)	0.03233(14)	0	0.0212(8)
Cu3[d]	0.0235(2)	0.5724(2)	0	0.0238(12)
Se1	0.00166(9)	0.18205(9)	0	0.0101(3)
Se2	0.28414(9)	0.71065(9)	0	0.0104(3)
Se3	0.18345(10)	0.00037(9)	0	0.0101(3)
Se4	0.12251(10)	0.39978(9)	0	0.0126(3)
Se5	0.40745(10)	0.11407(9)	0	0.0125(3)

Note. Refined occupancies are [a]0.937(7), [b]0.560(7), [c]0.862(8), [d]0.650(9).

TABLE 4
Atomic Coordinates[a] and Equivalent Isotropic Displacement Parameters for $RbSm_2Ag_3Se_5$

Atom	*y*	*z*	U_{eq}
Rb	0.43702(6)	0.2500	0.0149(2)
Sm	0.308620(19)	0.595560(17)	0.00838(14)
Ag1	0.16055(4)	0.2500	0.01227(17)
Ag2	0.08441(3)	0.53813(3)	0.01289(16)
Se1	0.06460(4)	0.11990(3)	0.00898(16)
Se2	0.75810(6)	0.2500	0.0093(2)
Se3	0.32140(4)	0.07123(3)	0.00850(17)

[a] The *x* coordinate of all atoms is 0.

The structure of $Rb_{1.5}Ln_2Cu_{2.5}Se_5$ (*Ln* = Gd, Dy), illustrated in Fig. 4, is also a three-dimensional tunnel structure.

TABLE 5
Selected Bond Distances (Å) for $RbSm_2CuSe_4$, $RbGd_2CuSe_4$, and $RbDy_2CuSe_4$

Compound	$RbSm_2CuSe_4$	$RbGd_2CuSe_4$	$RbDy_2CuSe_4$
Rb–Se1 × 4	3.4180(9)	3.4042(10)	3.3830(19)
Rb–Se2 × 2	3.3096(12)	3.2943(14)	3.266(3)
Rb–Se3 × 2	3.9347(8)	3.9272(8)	3.8959(13)
Ln–Se1 × 2	2.8782(6)	2.8581(7)	2.8292(13)
Ln–Se1	2.9095(9)	2.8956(10)	2.8571(18)
Ln–Se2	2.8593(7)	2.8456(7)	2.8218(12)
Ln–Se3 × 2	2.9812(5)	2.9665(5)	2.9385(8)
Cu–Se1 × 2	2.4672(10)	2.4675(12)	2.453(2)
Cu–Se2	2.4748(10)	2.4631(11)	2.449(2)

TABLE 6
Selected Bond Distances for $Rb_{1.5}Gd_2Cu_{2.5}Se_5$ and $Rb_{1.5}Dy_2Cu_{2.5}Se_5$

Compound	$Rb_{1.5}Gd_2Cu_{2.5}Se_5$	$Rb_{1.5}Dy_2Cu_{2.5}Se_5$
Rb1–Se1 × 2	3.5003(17)	3.4642(19)
Rb1–Se2 × 2	3.3307(15)	3.3007(17)
Rb1–Se3 × 2	3.5275(16)	3.4989(18)
Rb1–Se4	3.525(2)	3.521(2)
Rb1–Se5	3.770(2)	3.681(2)
Rb2–Se1 × 4	3.6016(12)	3.5945(13)
Rb2–Se3 × 4	3.5938(12)	3.5872(14)
*Ln*1–Se2	2.7695(15)	2.7399(17)
*Ln*1–Se3 × 2	2.8163(11)	2.7782(12)
*Ln*1–Se4	2.9759(16)	2.9622(17)
*Ln*1–Se5 × 2	3.0046(11)	2.9680(13)
*Ln*2–Se1 × 2	2.8010(11)	2.7719(12)
*Ln*2–Se2	2.7656(16)	2.7349(18)
*Ln*2–Se4 × 2	2.9986(11)	2.9665(12)
*Ln*2–Se5	3.0555(15)	3.0180(17)
Cu1–Se1	2.484(2)	2.468(2)
Cu1–Se2 × 2	2.5286(13)	2.5074(14)
Cu1–Se3	2.464(2)	2.453(2)
Cu2–Se4 × 2	2.4903(14)	2.4613(16)
Cu2–Se5	2.410(2)	2.412(3)
Cu2–Se5	2.896(3)	2.942(3)
Cu3–Se4	2.396(4)	2.398(4)
Cu3–Se5 × 2	2.4189(19)	2.413(2)

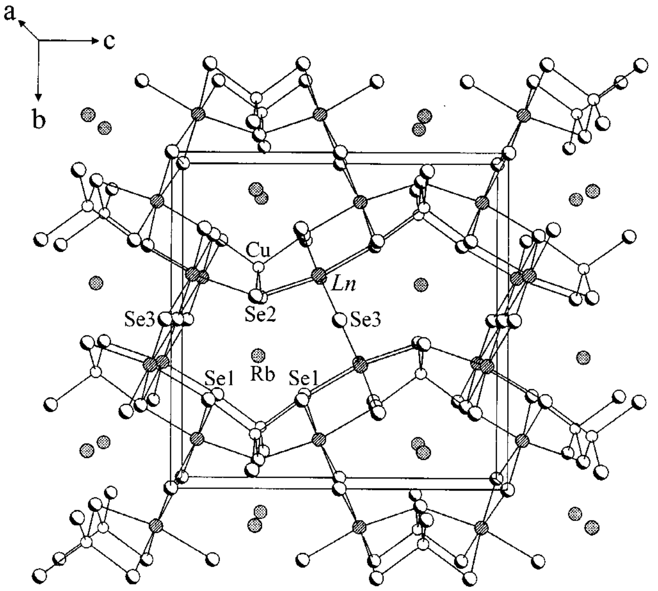

FIG. 1. The unit cell of $RbLn_2CuSe_4$ viewed down in [100].

Its structure is similar to that of $K_{1.5}Dy_2Cu_{2.5}Te_5$, but only three of the four tetrahedral Cu sites in $K_{1.5}Dy_2Cu_{2.5}Te_5$ (5) are occupied in the present structure. In one tunnel three Rb^+ cations are placed in a 20-membered ring composed of four Cu–Se bonds and 16 *Ln*–Se bonds. The three-dimensional anionic framework is also built from $LnSe_6$ octahedra and $CuSe_4$ tetrahedra. Infinite chains of vertex-sharing $CuSe_4$ tetrahedra (Cu1) are found again running along the [001] direction (see Figs. 4 and 2). Infinite double chains made up from these infinite chains by edge-sharing run in the [001] direction, as shown in Fig. 5a. Such double chains have been found not only in $K_{1.5}Dy_2Cu_{2.5}Te_5$ (5) but also in layered compounds $NaMCuQ_3$ (M = Ti, Zr; Q = S, Se, Te) (20), $TlTiCuTe_3$ (21), and $Na_2ZrCu_2Se_4$ (22). The $CuSe_4$ tetrahedra in these chains are distorted with Cu2–Se4 (× 2), Cu2–Se5, and Cu2–Se5 distances of 2.4613(16), 2.412(3), and 2.942(3) Å for $Rb_{1.5}Dy_2Cu_{2.5}Se_5$, as an example. Another potential tetrahedral site in the chain in Fig. 5b, which is partially occupied by a Cu atom in $K_{1.5}Dy_2Cu_{2.5}Te_5$, is distorted into a triangular site (one Se4, two Se5) about a Cu3 atom. In $Rb_{1.5}Ln_2Cu_{2.5}Se_5$ the Cu–Cu distances may range from 2.477(7) to 2.809(3) Å, but need not since the Cu2 and Cu3 sites are partially occupied. However, such $Cu^+(d^{10})$–$Cu^+(d^{10})$ interactions have been described elsewhere (5, 23–26).

$RbSm_2Ag_3Se_5$ is also a three-dimensional tunnel structure, as shown in Fig. 6. The tunnel is very similar to that in $RbLn_2CuSe_4$ and holds one Rb^+ cation in a 10-membered ring consisting of six Ag–Se bonds and four Sm–Se bonds. The framework is related to that in $RbLn_2CuSe_4$, being built from $LnSe_6$ octahedra and $AgSe_4$ tetrahedra. Figure 7 shows some of the single chains and double chains that share vertices in $RbSm_2Ag_3Se_5$.

Selected bond distances for these six compounds are listed in Tables 5, 6, and 7. The Rb^+ cations are coordinated to bicapped trigonal prisms of eight Se atoms in these

TABLE 7
Selected Bond Distances (Å) for $RbSm_2Ag_3Se_5$

Rb–Se1 × 4	3.6853(7)	Sm–Se3 × 2	2.9616(5)
Rb–Se2 × 2	3.4777(11)	Ag1–Se1 × 2	2.6966(8)
Rb–Se3 × 2	3.5773(9)	Ag1–Se2 × 2	2.6225(7)
Sm–Se1 × 2	2.9289(5)	Ag2–Se1	2.6792(8)
Sm–Se2	2.8758(6)	Ag2–Se1	2.7693(8)
Sm–Se3	2.9120(8)	Ag2–Se3 × 2	2.6572(5)

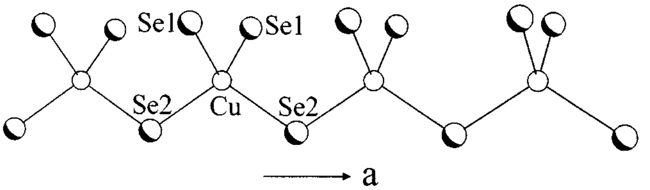

FIG. 2. The vertex-shared infinite $CuSe_4$ chain in the [100] direction in $RbLn_2CuSe_4$.

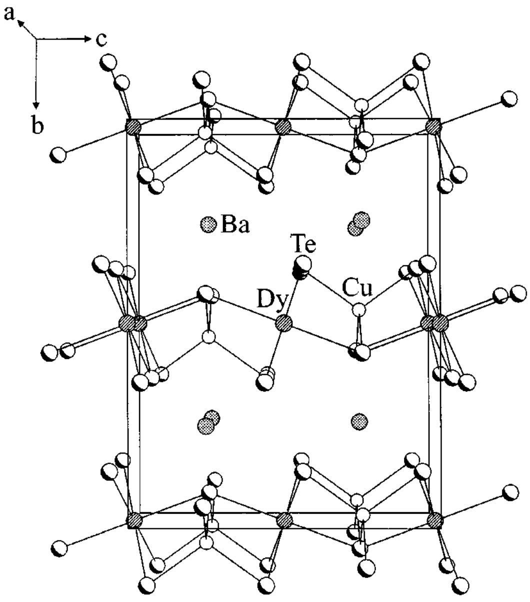

FIG. 3. The unit cell of $BaDyCuTe_3$ (5) viewed down [100].

structures, with Rb–Se distance ranging from 3.266(3) to 3.9347(8) Å, consistent with those in Rb_2Se_5 (3.36(2)–3.74(2) Å) (27). *Ln*–Se distances are unexceptional and decrease from Sm to Gd to Dy, as is expected given the lanthanide contraction.

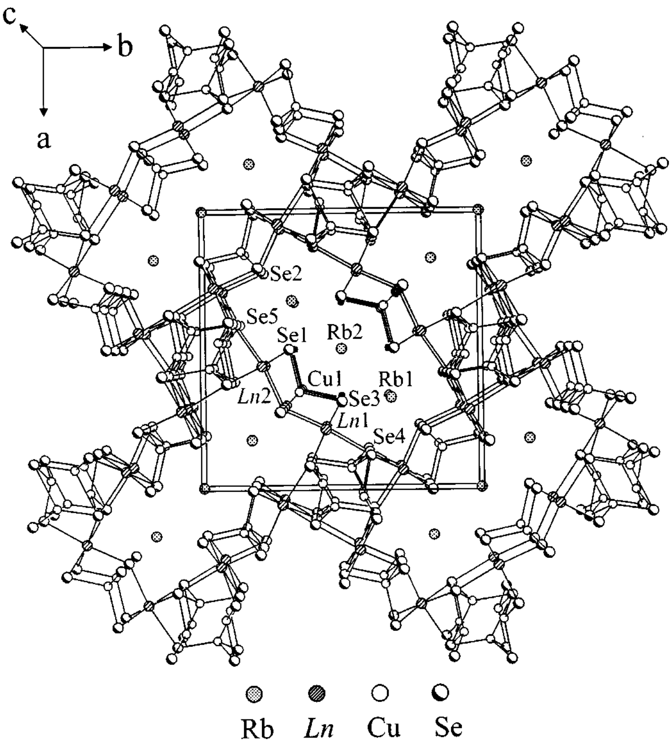

FIG. 4. The unit cell of $Rb_{1.5}Ln_2Cu_{2.5}Se_5$ viewed down [001]. The Cu2 and Cu3 sites (see Fig. 5) are not labeled for the sake of clarity.

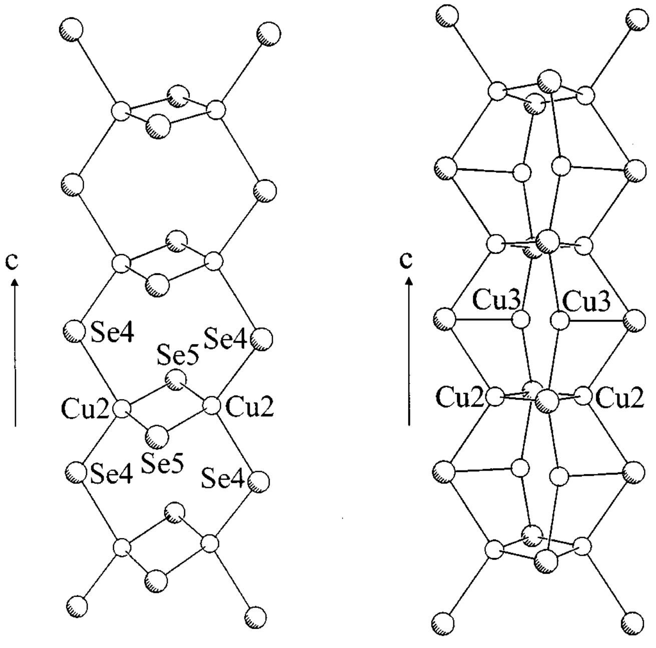

(a) (b)

FIG. 5. (a) The double chain made up from two infinite chains in Fig. 2 by edge-sharing in the [001] direction; (b) the double chain with the triangularly coordinated Cu3 atoms.

A plot of $1/\chi$ vs T is shown in Fig. 8 for $Rb_{1.5}Dy_2Cu_{2.5}Se_5$ This material is paramagnetic in the 5–300 K range. The susceptibility data were fit by a least-squares

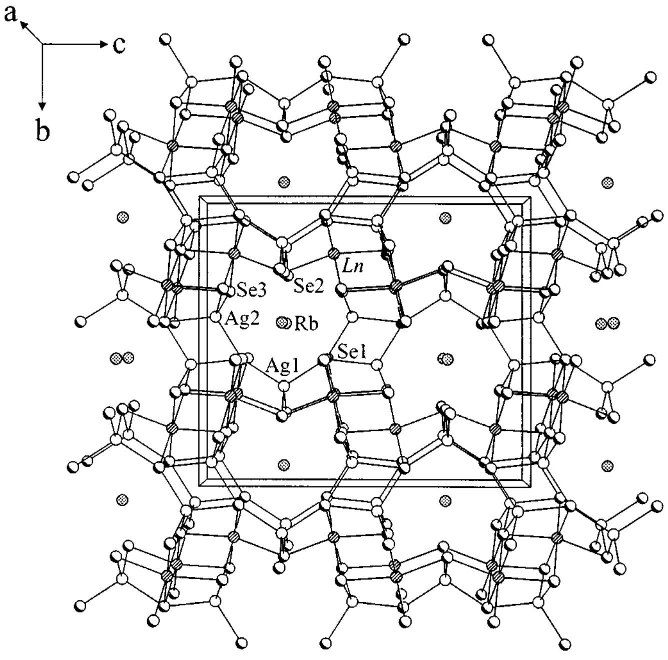

FIG. 6. The unit cell of $RbSm_3Ag_2Se_5$ viewed down [100].

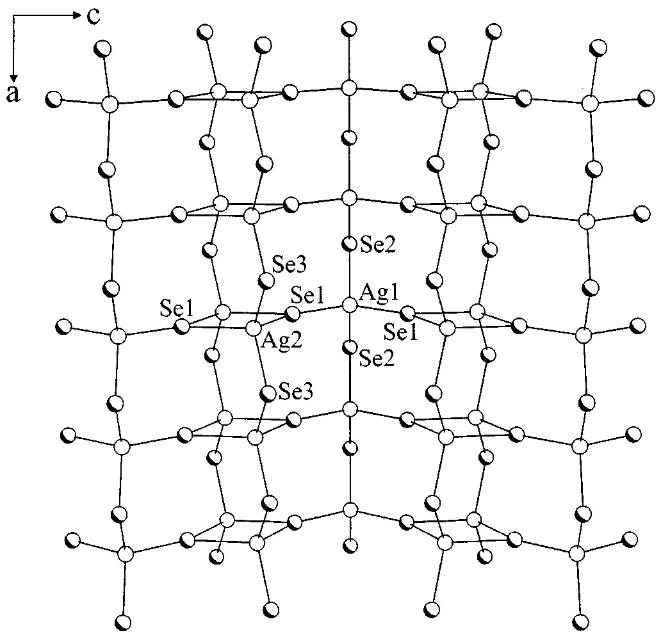

FIG. 7. Part of the structure of $RbSm_3Ag_2Se_5$ viewed in the (101) plane.

method to the Curie–Weiss equation $\chi = C/(T - \theta)$, where C is the Curie constant and θ is the Weiss constant. The resulting values for C and θ are 14.10(5) emuKmol^{-1} and $-11.23(7)$ K, respectively. The calculated effective magnetic moment of 10.63(4) μ_B agrees well with the theoretical value of 10.65 μ_B for Dy^{3+} (28).

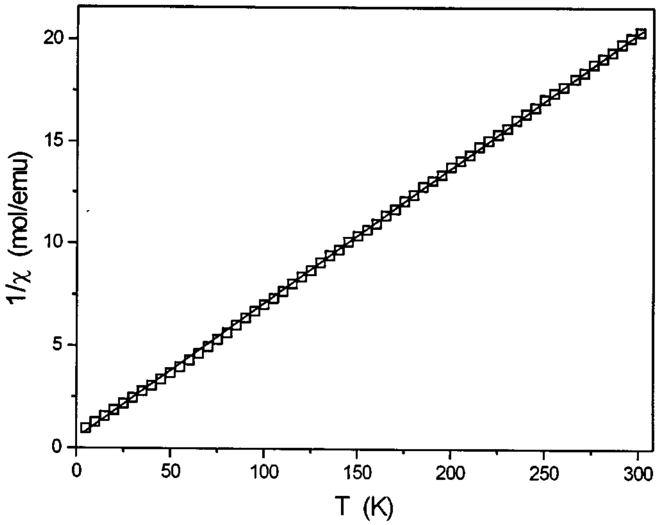

FIG. 8. Plot of the molar susceptibility $1/\chi$ vs T for $Rb_{1.5}Dy_2Cu_{2.5}Se_5$, where the solid line is the least-squares fit.

ACKNOWLEDGMENTS

Use of the X-ray, scanning electron microscope, and magnetic susceptibility facilities was supported by the National Science Foundation through the Northwestern University Materials Research Center, Grant DMR96-32472. This research was supported by the National Science Foundation through Grant DMR 97-09351.

REFERENCES

1. J. A. Cody and J. A. Ibers, *Inorg. Chem.* **34,** 3165 (1995).
2. A. E. Christuk, P. Wu, and J. A. Ibers, *J. Solid State Chem.* **110,** 330 (1994).
3. P. Wu, A. E. Christuk, and J. A. Ibers, *J. Solid State Chem.* **110,** 337 (1994).
4. P. Wu and J. A. Ibers, *J. Alloys Compd.* **229,** 206 (1995).
5. F. Q. Huang, W. Choe, S. Lee, and J. S. Chu, *Chem. Mater.* **10,** 1320 (1998).
6. P. Wu and J. A. Ibers, *Z. Kristallogr.* **208,** 35 (1993).
7. P. Stoll, P. Dürichen, C. Näther, and W. Bensch, Z. *Anorg. Allg. Chem.* **624,** 1807 (1998).
8. A. C. Sutorik, J. Albritton-Thomas, C. R. Kannewurf, and M. G. Kanatzidis, *J. Am. Chem. Soc.* **116,** 7706 (1994).
9. W. Bensch and P. Dürichen, *Chem. Ber.* **129,** 1489 (1996).
10. A. C. Sutorik, J. Albritton-Thomas, T. Hogan, C. R. Kannewurf, and M. G. Kanatzidis, *Chem. Mater.* **8,** 751 (1996).
11. R. Patschke, P. Brazis, C. R. Kannewurf, and M. Kanatzidis, *Inorg. Chem.* **37,** 6562 (1998).
12. R. Patschke, J. Heising, and M. Kanatzidis, *Chem. Mater.* **10,** 695 (1998).
13. R. Patschke, P. Brazis, C. R. Kannewurf, and M. Kanatzidis, *J. Mater. Chem.* **8,** 2587 (1998).
14. S. A. Sunshine, D. Kang, and J. A. Ibers, *J. Am. Chem. Soc.* **109,** 6202 (1987).
15. "SMART, Version 5.054," data collection and "SAINT-Plus, Version 6.0," data processing software for the SMART system. Bruker Analytical X-Ray Instruments, Inc., Madison, WI, 1999.
16. G. M. Sheldrick, "SHELXTL DOS/Windows/NT Version 5.10." Bruker Analytical X-Ray Instruments, Inc., Madison, WI, 1977.
17. L. N. Mulay and E. A. Boudreaux (Eds.), "Theory and Applications of Molecular Diamagnetism." Wiley–Interscience, New York, 1976.
18. M. F. Mansuetto, P. M. Keane, and J. A. Ibers, *J. Solid State Chem.* **101,** 257 (1992).
19. M. A. Pell and J. A. Ibers, *Chem. Ber.* **130,** 1 (1997).
20. M. F. Mansuetto, P. M. Keane, and J. A. Ibers, *J. Solid State Chem.* **105,** 580 (1993).
21. M. A. Pell and J. A. Ibers, *J. Alloys Compd.* **240,** 37 (1996).
22. M. F. Mansuetto and J. A. Ibers, *J. Solid State Chem.* **117,** 30 (1995).
23. N.-H. Dung, M.-P. Pardo, and P. Boy, *Acta Crystallogr., Sect. C: Cryst. Struct. Commun.* **39,** 668 (1983).
24. K. Yvon, A. Paoli, R. Flükiger, and R. Chevrel, *Acta Crystallogr., Sect. B: Struct. Crystallogr. Cryst. Chem.* **33,** 3066 (1977).
25. H. Li, R. Mackay, S.-J. Hwu, Y.-K. Kuo, M. J. Skove, Y. Yokota, and T. Ohtani, *Chem. Mater.* **10,** 3172 (1998).
26. S.-J. Hwu, H. Li, R. Mackay, Y.-K. Kuo, M. J. Skove, M. Mahapatro, C. K. Bucher, J. P. Halladay, and M. W. Hayes, *Chem. Mater.* **10,** 6 (1998).
27. K.-J. Range and R. Leeb, *Z. Naturforsch., B: Anorg. Chem., Org. Chem.* **31,** 685 (1976).
28. W. E. Hatfield, *in* "Solid State Chemistry: Techniques" (A. K. Cheetham and P. Day, Eds.), pp. 122–162, Clarendon Press, New York, 1987.